The FASEB Journal article fj.201700482R. Published online October 6, 2017.

THE FASEB JOURNAL • RESEARCH • www.fasebj.org

Cell-specific expression of runt-related transcription factor 2 contributes to pulmonary fibrosis

Carlo Mümmler,* Olivier Burgy,† Sarah Hermann,* Kathrin Mutze,* Andreas Günther,‡ and Melanie Königshoff*,†,1

*Comprehensive Pneumology Center, Helmholtz Center Munich, University Hospital Grosshadern, Ludwig Maximilians University München, Munich, Germany; †Division of Pulmonary Sciences and Critical Care Medicine, Department of Medicine, University of Colorado, Denver, Colorado, USA; and ‡Department of Internal Medicine, University of Giessen Lung Center, Giessen, Germany

ABSTRACT: Idiopathic pulmonary fibrosis (IPF) is a fatal lung disease with limited therapeutic options and unknown etiology. IPF is characterized by epithelial cell injury, impaired cellular crosstalk between epithelial cells and fibroblasts, and the formation of fibroblast foci with increased extracellular matrix deposition (ECM). We investigated the role of runt-related transcription factor 2 (RUNX2), a master regulator of bone development that has been linked to profibrotic signaling. RUNX2 expression was up-regulated in lung homogenates from patients with IPF and in experimental bleomycin-induced lung fibrosis. The RUNX2 level correlated with disease severity as measured by decreased diffusing capacity and increased levels of the IPF biomarker, matrix metalloproteinase 7. Nuclear RUNX2 was observed in prosurfactant protein C–positive hyperplastic epithelial cells and was rarely found in myofibroblasts. We discovered an up-regulation of RUNX2 in fibrotic alveolar epithelial type II (ATII) cells as well as an increase of RUNX2-negative fibroblasts in experimental and human pulmonary fibrosis. Functionally, small interfering RNA–mediated RUNX2 knockdown decreased profibrotic ATII cell function, such as proliferation and migration, whereas fibroblasts displayed activation markers and increased ECM expression after RUNX2 knockdown. This study reveals that RUNX2 is differentially expressed in ATII cells *vs.* fibroblasts in lung fibrosis, which contributes to profibrotic cell function. Cell-specific targeting of RUNX2 pathways may represent a therapeutic approach for IPF.—Mümmler, C., Burgy, O., Hermann, S., Mutze, K., Günther, A., Königshoff, M. Cell-specific expression of runt-related transcription factor 2 contributes to pulmonary fibrosis. FASEB J. 32, 000–000 (2018). www.fasebj.org

KEY WORDS: RUNX2 · IPF · alveolar epithelial cells · fibroblast

Idiopathic pulmonary fibrosis (IPF) is a fatal interstitial lung disease of as-yet-unknown etiology that occurs predominantly in aged, male patients (1). Patients usually suffer from cough and dyspnea and exhibit gradual lung function decline that finally leads to respiratory failure (2). Our current pathophysiologic knowledge suggests that perpetuated injuries to the distal lung lead to impaired alveolar wound repair and hyperplastic alveolar epithelial cells, often overlying activated myofibroblasts (3, 4). These myofibroblasts form so-called fibroblastic foci with increased deposition of extracellular matrix (ECM) (3). It has been demonstrated that disturbed epithelial–mesenchymal crosstalk is driven *via* epithelial secretion of different growth factors, such as TGF-β and PDGF, as well as *via* the reactivation of developmental pathways, such as WNT, sonic hedgehog, or Notch (3, 5). Although two drugs have recently been approved for therapy, the prognosis of IPF remains poor. Nintedanib and pirfenidone are able to reduce lung function decline; however, neither reverse or stop the disease (6, 7). Thus, a better understanding of IPF pathophysiology and the identification of novel targets are urgently needed to design more effective treatments for the future.

Runt-related transcription factors (RUNXs) comprise a family of genes that are fundamental for organ development and play important roles in tumor formation and progression. RUNX proteins can act as both tumor suppressor genes or dominant oncogenes, depending on the cellular context (8). The three RUNX genes share the highly

ABBREVIATIONS: ACTB, β-actin; ATII, alveolar epithelial type II; BLEO, bleomycin; CBFB, core-binding factor, β-subunit; COL1, collagen 1; DLCO, diffusing capacity of the lung for carbon monoxide; ECM, extracellular matrix; IPF, idiopathic pulmonary fibrosis; MMP, matrix metalloprotease; phLF, primary human lung fibroblast; proSPC, prosurfactant protein C; RUNX, runt-related transcription factor; siRNA, small interfering RNA; αSMA, α-smooth muscle actin

[1] Correspondence: Division of Pulmonary Sciences and Critical Care Medicine, Department of Medicine, University of Colorado, AMC, Research 2, 9th Floor, 12700 East 19th Ave., Denver, CO 80045, USA. E-mail: melanie.koenigshoff@ucdenver.edu

doi: 10.1096/fj.201700482R

This article includes supplemental data. Please visit *http://www.fasebj.org* to obtain this information.

homologous runt domain, which is essential for DNA binding and interaction with the coactivator, core-binding factor, β-subunit (CBFB) (9, 10). RUNX factors are scaffolding proteins that bind DNA after complexing with CBFB. In the nucleus, the RUNX/CBFB complex can interact with a variety of cofactors, such as Lef1, Smad, or p300, that determine the outcome of RUNX-mediated gene transcription (11, 12). Knockout mice show distinct phenotypes, with respiratory failure reported for RUNX2- and RUNX3-null mice (13–15). Of importance, several lines of evidence indicate crosstalk of RUNX transcription factors with profibrotic signaling pathways, such as TGF-β, bone morphogenetic protein, or WNT signaling (8, 16), which have been shown to be critically involved in IPF (5). TGF-β signaling can induce RUNX2 expression or alter its DNA binding activity. RUNX2 can also interact with TGF-β signaling *via* modulation of downstream signaling molecules, such as Smad3 or the TGF-β type I receptor (17). Moreover, it has been demonstrated that canonical WNT/β-catenin signaling activates the RUNX2 promoter and induces its expression (18). Modulation of RUNX2 activity by these fibrosis-associated signaling pathways led us to hypothesize that RUNX2 might be involved in pulmonary fibrosis. In this study, we report that RUNX2 is differentially expressed in fibrotic alveolar epithelial cells and fibroblasts, which contributes to profibrotic cellular function and promotes the progression of lung fibrosis.

MATERIALS AND METHODS

Animals and bleomycin administration

All animal experiments were approved by the Government of Upper Bavaria and registered under Project 55.2-1-54-2532-88-12. Eight- to 10-wk-old C57BL/6N mice (Charles River Laboratories, Sulzfeld, Germany) were housed under standard conditions and had free access to water and laboratory rodent chow. For the induction of pulmonary fibrosis, mice were instilled with 3 U/kg body weight bleomycin sulfate (Almirall, Barcelona, Spain) dissolved in 50 μl sterile PBS (Thermo Fisher Scientific, Waltham, MA, USA). Control mice were instilled with 50 μl sterile PBS. Intratracheal instillation was performed by using a Micro-Sprayer Aerosolizer (Model IA-1C; Penn Century, Wyndmoor, PA, USA). Mice were humanely killed, and lungs were excised, flushed with saline, snap frozen, and stored until analysis.

Primary cell isolation

Primary murine alveolar epithelial type II (pmATII) cells were isolated as published previously (19). In brief, mouse lungs were harvested after bronchoalveolar lavage was performed and flushed with 0.9% NaCl solution through the right heart. Lungs were inflated with 1.5 ml dispase (BD Biosciences, San Jose, CA, USA) and subsequently perfused with 300 μl of 1% low-melting-point agarose (Sigma-Aldrich, St. Louis, MO, USA). Agarose-filled lungs were incubated for 45 min at room temperature. Lungs were then minced and filtered through nylon meshes with pore sizes of 100, 20, and 10 μm (Sefar, Heiden, Switzerland). Samples were centrifuged at 200 *g* for 10 min. Pellet was resuspended and the resulting cell suspension was incubated in petri dishes coated with Abs against CD45 and CD16/32 for a negative selection of macrophages and lymphocytes. Negative selection for fibroblasts was performed by adherence on cell culture dishes for 25 min. After a viability check with trypan blue, cells were either snap frozen in liquid nitrogen for additional RNA or protein isolation or seeded in DMEM medium (Thermo Fisher Scientific) that contained 10% fetal bovine serum (FBS; PAN Biotech, Aidenbach, Germany), 2 mM L-glutamine (Thermo Fisher Scientific), 3.6 mg/ml glucose, 10 mM HEPES (Thermo Fisher Scientific), and 1% penicillin/streptomycin (Thermo Fisher Scientific).

Isolation of primary human lung fibroblasts (phLFs) was approved by the local ethics committee of the Ludwig Maximilians University München (333-10). phLFs were isolated as published previously (20). In brief, specimens of lung resections were cut in 1- to 2-cm^2 pieces and digested with collagenase I (Biochrom, Cambridge, United Kingdom) at 37°C for 2 h. Digested material was filtered through nylon filters with a pore size of 70 μm. After centrifugation at 400 *g* and 4°C for 5 min, cells were cultured under standard conditions, at 37°C, 5% CO_2 using DMEM/nutrient mixture F12 medium (DMEM/F12; Thermo Fisher Scientific) that was supplemented with 20% FBS and 1% penicillin/streptomycin.

Cell culture and transfection

Alveolar epithelial A549 cells (CCL-185; American Type Culture Collection, Manassas, VA, USA) were cultured in DMEM/F-12 (Thermo Fisher Scientific) that was supplemented with 10% FBS. After starvation in DMEM + 0.1% FBS, cells were stimulated with recombinant human TGF-β1 (R&D Systems, Minneapolis, MN, USA) or glycogen synthase kinase 3 inhibitor, CHIR 99021 (R&D Systems), at indicated doses for 24 h.

RUNX2 or scrambled control small interfering RNA (siRNA) were transfected by using Lipofectamine RNAiMax (Thermo Fisher Scientific). For pmATII cells, freshly isolated cells were plated in 12-well plates in a density of 1 million cells per well. On d 2 after isolation, cells were transfected with 80 nM of a pool of 3 siRNAs that targeted murine RUNX2 mRNA or scrambled control siRNA. For phLFs, cells at passages 5–8 were reverse transfected with 20 nM siRNA that targeted human RUNX2 mRNA or scrambled control siRNA. A549 at passages 5–7 were used for RUNX2 silencing experiments and siRNA that targeted human RUNX2 mRNA was used at a final dose of 50 nM. siRNA used was for murine RUNX2 mRNA (Santa Cruz Biotechnology, Dallas, TX, USA), human RUNX2 mRNA (Santa Cruz Biotechnology), and scrambled control siRNA (Santa Cruz Biotechnology). Cells were examined 48 h post-transfection, which reflects d 4 after isolation for pmATII cells.

Human tissue

Whole-lung homogenates of patients with IPF or healthy donor—lung explants not used for transplantation—were used for RNA isolation and protein isolation. Paraffin-embedded tissue sections were used for immunofluorescent staining. All lung tissue samples were collected in frame of the European IPF registry and provided by the University of Giessen Lung Center Giessen Biobank [member of the German Center for Lung Research (DZL) Platform Biobanking]. Study protocol was approved by the Ethics Committee of the Justus-Liebig-University Giessen (111/08 and 58/15).

Immunofluorescence staining

Lung sections of patients with IPF and donors or bleomycin (BLEO)- and PBS-treated murine lungs were deparaffinized before an antigen retrieval step was performed in a pressure cooker at 125°C. Sections were permeabilized with 0.1% Triton X-100 (AppliChem, Darmstadt, Germany) for 15 min and blocked with 5% bovine serum albumin (Sigma-Aldrich) for 1 h. RUNX2 Ab (Abcam, Cambridge, United Kingdom), α-smooth muscle actin

(αSMA) Ab (Abcam), pro-surfactant protein C (proSPC) Ab (EMD Millipore, Darmstadt, Germany), or cytokeratin (CK) Ab (Dako, Hamburg, Germany) were diluted in Ab diluent (Zytomed Systems, Berlin, Germany) and applied to lung sections overnight on 4°C. Fluorophore-labeled secondary Ab (Thermo Fisher Scientific) was applied for 1 h at room temperature. DAPI (Sigma-Aldrich) was applied to visualize cell nuclei. Slides were mounted with fluorescence mounting medium (Dako). Digital images were obtained by using an Axioimager Microscope (Zeiss, Oberkochen, Germany). All images presented in the same panel were captured by using identical detector settings. Semiquantitative analysis has been performed by using ImageJ (National Institutes of Health, Bethesda, MD, USA) on at least 3 images per sample.

RNA isolation and cDNA synthesis

Mouse lungs were homogenized by using a Sartorius Micro-Dismembrator S (Thermo Fisher Scientific). Subsequently, total RNA was isolated by using phenol-chloroform extraction and the peqLab Gold Total RNA Kit (PEQLAB; VWR International GmbH, Erlangen, Germany). RNA from murine ATII cells and primary human lung fibroblasts was isolated by using peqLab Gold Total RNA Kit according to manufacturer instructions. RNA concentration and purity were determined by using a Nano-Drop spectrophotometer (Thermo Fisher Scientific). One thousand nanograms of total RNA was applied for cDNA synthesis by using the SuperScriptII Kit (Thermo Fisher Scientific) and a Mastercycler nexus (Eppendorf, Hamburg, Germany).

Quantitative RT-PCR

Quantitative RT-PCR was performed in a LC480 II Lightcycler (Roche Diagnostics, Mannheim, Germany) using SYBR green (Roche Diagnostics). Primers (Eurofins Genomics, Ebersberg, Germany) are listed in **Table 1** (murine primers) and **Table 2** (human primers). Hypoxanthine guanine phosphoribosyl transferase (HPRT) was used as a reference gene. Cycle threshold (ΔC_t) values were calculated as follows: ΔC_t (gene of interest) = C_t (HPRT) – C_t (gene of interest). Fold changes were calculated by using the $2^{-\Delta\Delta Ct}$ method.

Protein isolation

Lung tissue was homogenized by using a Sartorius Micro-Dismembrator S. Tissue powder was then lysed in modified RIPA buffer (20 mM Tris HCl, 150 mM NaCl, 1 mM EDTA, 1 mM EGTA, 1% NP-40, 2.5 mM $Na_4P_2O_7$, 1% sodium deoxycholate). pmATII cells were washed with ice-cold PBS and frozen at −80°C. After lysing cells with T-Per (Thermo Fisher Scientific) and centrifugation at 15,000 *g* for 30 min, supernatant was collected and protein concentration was determined [bicinchoninic acid (BCA); Thermo Fisher Scientific]. phLFs were lysed with modified RIPA, centrifuged at 15,000 *g* for 30 min, and the supernatant was used for BCA and Western blot analysis.

Scratch assay

A549 cells were seeded in 6-well plates at a confluence of 80%, transfected with siRUNX2 or control as previously outlined, and starved for 12 h. Confluent monolayers were wounded by scraping a pipette tip across the monolayer, as previously described (21). After washing with PBS, cells were cultured in DMEM + 0.1% FBS. Images were captured immediately after the scratch (t = 0 h), then observed 24 and 48 h after the scratch by using a Moticam 1080 BMH camera (Motic, Kowloon Bay, Hong Kong) that was mounted on an inverted microscope with a ×4 objective (VWR International). Each condition was conducted in triplicate, and 3 areas were observed for each well. Images were blindly analyzed for the wound area by using ImageJ, and data were expressed as the percentage of wound closure normalized to t = 0 h.

Western blotting

Fifteen micrograms of protein lysate was run on SDS-PAGE gels and transferred to nitrocellulose membranes (Biozym Scientific, Hessisch Oldendorf, Germany). Roti-Block blocking solution (Carl Roth, Karlsruhe, Germany) was applied to the membrane for 1 h. Overnight incubation with Abs against RUNX2 (Abcam and MBL International, Woburn, MA, USA), αSMA (Sigma-Aldrich), collagen 1 (COL1; Rockland, Limerick, PA, USA), and β-actin (ACTB; Sigma-Aldrich), diluted in blocking solution, was performed at 4°C. After washing, horseradish peroxidase–conjugated secondary Ab (GE Healthcare, Chalfont St. Giles, United Kingdom) was applied for 1 h. Proteins of interest were detected with a ChemiDoc XRS+ system (Bio-Rad, Hercules, CA, USA) and Pierce ECL Substrate (Thermo Fisher Scientific) or SuperSignal West Dura Chemiluminescent Substrate (Thermo Fisher Scientific). Densitometric analysis was performed by using Image Lab software (v.4.0.1; Bio-Rad).

Statistical analysis

Statistical analysis was performed by using Prism 5 (GraphPad Software, La Jolla, CA, USA). Unpaired Student's t test or

TABLE 1. *List of murine primers*

Gene	Sequence, 5′–3′ Forward	Reverse	Product length (bp)
Acta2	GCTGGTGATGATGCTCCCA	GCCCATTCCAACCATTACTCC	81
Cbfb	TAAGTACACGGGCTTCAGGG	AAGTATACGATCTCCGAGCGA	93
Ccnd1	ATGCCAGAGGCGGATGAGA	ATGGAGGGTGGGTTGGAAAT	104
Col1a1	CCAAGAAGACATCCCTGAAGTCA	TGCACGTCATCGCACACA	129
Fn1	GGTGTAGCACAACTTCCAATTACG	GGAATTTCCGCCTCGAGTCT	92
Hprt	CCTAAGATGAGCGCAAGTTGAA	CCACAGGACTAGAACACCTGCTAA	86
Runx1	CATCGCTTTCAAGGTGGTGG	CGCGGTAGCATTTCTCAGTT	109
Runx2	ACGAGGCAAGAGTTTCACCT	TGTCTGTGCCTTCTTGGTTC	120
Runx3	TCTGAACCCAACCCCCTGA	TGCTCGGGTCTCGTATGAAG	117
S100a4	AGGAGCTACTGACCAGGGAGCT	TCATTGTCCCTGTTGCTGTCC	103
Tnc	GGCCCCGGCTTGAAGA	GGGCTTGAACCAGGTGATCA	105

TABLE 2. *List of human primers*

Gene	Sequence, 5′–3′ Forward	Reverse	Product length (bp)
ACTA2	GAGATCTCACTGACTACCTCATGA	AGAGCTACATAACACAGTTTCTCCTTGA	116
CCND1	CCGAGAAGCTGTGCATCTACAC	AGGTTCCACTTGAGCTTGTTCAC	94
COL1A1	CAAGAGGAAGGCCAAGTCGAG	TTGTCGCAGACGCAGATCC	128
FN1	CCGACCAGAAGTTTGGGTTCT	CAATGCGGTACATGACCCCT	81
HPRT	AAGGACCCCACGAAGTGTTG	GGCTTTGTATTTTGCTTTTCCA	157
RUNX1	TTCACAAACCCACCGCAAGT	TCTGCCGATGTCTTCGAGGTTC	88
RUNX2	TATGAGAGTAGGTGTCCCGC	TGCCTGGGGTCTGTAATCTG	102
S100A4	TCTTGGTTTGATCCTGACTGC	AACTTGTCACCCTCTTTGCC	105
TNC	CCATCTATGGGGTGATCCGG	TCGGTAGCCATCCAGGAGAG	139

Mann-Whitney *U* test were used (2-tailed, 95% CIs). Results are shown as means ± SEM.

RESULTS

RUNX2 is increased in IPF

We first examined the expression of RUNX2 in explanted lungs of patients with IPF and donor controls. Quantitative PCR analysis of whole-lung homogenate from donors or patients with IPF revealed that *RUNX2* mRNA was significantly increased in fibrotic lungs compared with donor lungs (donors: ΔC_t −0.58 ± 0.18 SEM; patients with IPF: ΔC_t 0.79 ± 0.15 SEM; $P < 0.0001$; **Fig. 1*A***). Next, protein levels of RUNX2, αSMA, and ACTB were assessed by Western blotting. RUNX2 protein expression was significantly increased (IPF fold-change: 1.53 ± 0.11 SEM; $P < 0.05$) and accompanied by increased levels of αSMA (Fig. 1*B*). To validate these findings in a larger cohort, we extracted the gene expression data of donors and patients with IPF from a Lung Tissue Research Consortium data set [Gene Expression Omnibus Series (GSE) accession number:

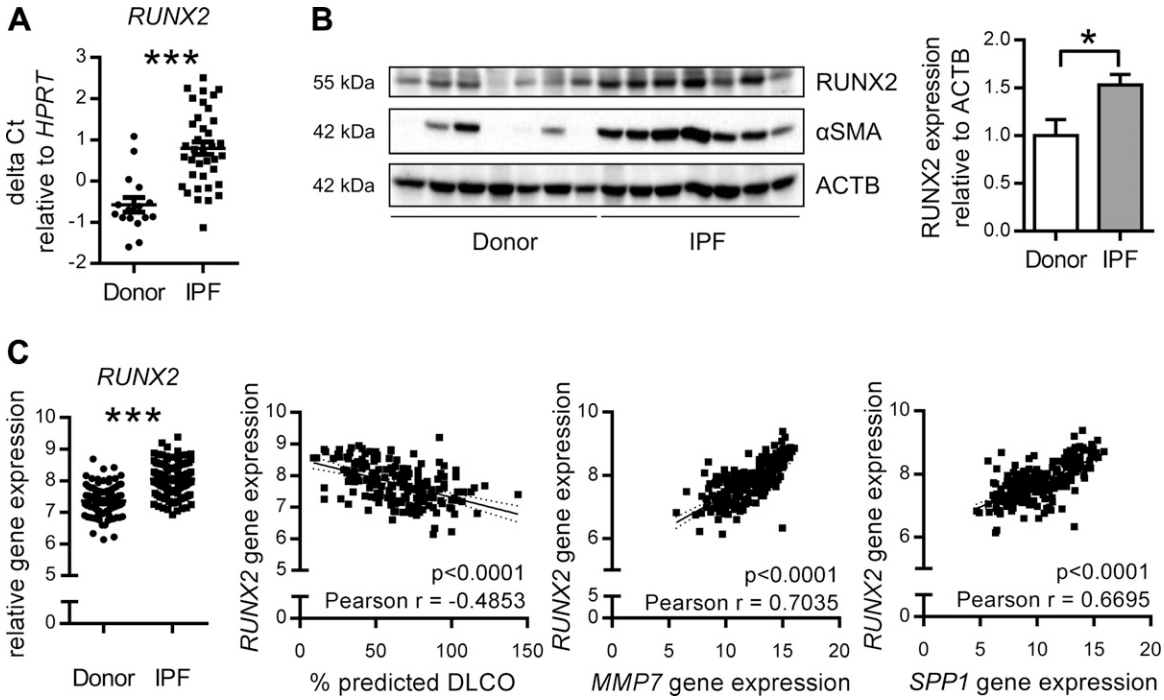

Figure 1. RUNX2 expression is increased in idiopathic pulmonary fibrosis. *A*) mRNA levels of *RUNX2* were assessed by qPCR in whole lung homogenate of donors and IPF patients. Data was normalized to Hypoxanthin-Guanin-Phosphoribosyltransferase (*HPRT*) and is shown as ΔC_t, means ± SEM. $n = 16$ for donors, $n = 37$ for IPF patients. *B*) Protein expression of RUNX2 and αSMA was determined in whole lung homogenates of donors and IPF patients. Densitometric analysis was performed using β-Actin (ACTB) as loading control; $n = 7$ donors, $n = 7$ IPF patients. *C*) Analysis of microarray data published with the accession number GSE47460 by the Lung Genomics Research Consortium. Gene expression levels of *RUNX2* were assessed in donors and IPF patients. Gene expression was correlated with % predicted diffusing capacity for carbon monoxide (DLCO) or expression levels of potential IPF biomarkers matrix metalloproteinase-7 (*MMP7*) and osteopontin (*SPP1*); $n = 91$ for donors, $n = 122$ for IPF patients. Statistics: unpaired Student's *t* test (*A*) and Mann-Whitney *U* test (*B*). Spearman *r* was used for correlation analysis (*C*). $^*P < 0.05$, $^{***}P < 0.001$.

47460; National Center for Biotechnology Information, Bethesda, MD, USA; *https://www.ncbi.nlm.nih.gov/geo/*]. Here, we confirmed the up-regulation of *RUNX2* mRNA in the lungs of patients with IPF compared with healthy donors (relative gene expression: donors: 7.37 ± 0.05 SEM; patients with IPF: 8.05 ± 0.05 SEM; $P < 0.001$; Fig. 1*C*). Of note, *RUNX2* levels were negatively correlated with the diffusing capacity of the lung for carbon monoxide (DLCO; Spearman $r = -0.49$; $P < 0.0001$). Furthermore, *RUNX2* levels were positively correlated with matrix metalloproteinase 7 (*MMP7*) and osteopontin (*SPP1*), potential biomarkers for IPF (Spearman $r = 0.70$; $P < 0.0001$; and Spearman $r = 0.67$; $P < 0.0001$, respectively) (22). The main binding partner of RUNT-related genes, *CBFB*, was also increased in human pulmonary fibrosis (relative gene expression: donors: 10.63 ± 0.03 SEM; patients with IPF: 10.79 ± 0.01 SEM; $P < 0.001$; Supplemental Fig. 1) and correlated with DLCO and IPF biomarkers (correlation with DLCO: Spearman $r = -0.26$; $P < 0.0001$; correlation with *MMP7*: Spearman $r = 0.37$; $P < 0.0001$; correlation with *SPP1*: Spearman $r = 0.38$; $P < 0.0001$; Supplemental Fig. 1).

RUNX2 is expressed in several cell types and colocalizes with proSPC-positive hyperplastic ATII cells

To identify which cells express RUNX2 in the human lung, we performed costaining on lung sections of donors and patients with IPF together with proSPC as an ATII cell marker or αSMA as a myofibroblast and smooth muscle cell marker. Hyperplastic ATII cells of patients with IPF exhibited a strong signal for RUNX2, whereas we detected less RUNX2 nuclear–positive ATII cells in donors (**Fig. 2*A***). Only a few αSMA-positive myofibroblasts exhibited nuclear RUNX2 in IPF lungs compared with donors (Fig. 2*A*). To further assess the cellular distribution of RUNX2, we quantified the number of RUNX2-positive cells that expressed proSPC or αSMA in IPF and donor lung tissue specimens (Fig. 2*B* and Supplemental Table 1). We found a significant increase in double-positive proSPC/RUNX2 cells in IPF compared with donor lungs (Fig. 2*B* and Supplemental Table 1) with hyperplastic RUNX2-positive ATII cells often in close proximity to αSMA-positive myofibroblast foci (Fig. 2*C*).

Surprisingly, however, within αSMA-positive cells, we primarily observed an increase in the RUNX2-negative subpopulation in IPF compared with donor lungs, which indicated that differential cell-specific RUNX2 expression might contribute to pulmonary fibrosis (Fig. 2*B*).

RUNX2 mRNA and protein levels are increased in experimental pulmonary fibrosis

We also assessed RUNX2 expression in experimental lung fibrosis. Intratracheal administration of bleomycin is one of the most commonly used models of pulmonary fibrosis in mice (23). Bleomycin injury leads to an acute inflammatory process that peaks at approximately d 7 and subsequently evolves into fibrotic lung remodeling at around d 14, recapitulating many aspects of human pulmonary fibrosis (23). Murine lung fibrosis was confirmed at d 14 by a reduction in lung function (Supplemental Fig. 2*A*). Moreover, lung histology revealed distorted tissue architecture and extracellular matrix remodeling (Supplemental Fig. 2*B*), as well as increased mRNA expression of the fibrotic markers, collagen1α1 (*Col1a1*), tenascin-C (*Tnc*), and fibronectin (*Fn1*; Supplemental Fig. 2*C*). We assessed the mRNA levels of *Runx* factors and their main interaction partner, *Cbfb*, at 14 d after bleomycin challenge (**Fig. 3*A***). *Runx2* was significantly up-regulated on the mRNA level in bleomycin-induced fibrosis (PBS: ΔC_t −1.63 ± 0.19 SEM; BLEO: −0.94 ± 0.17 SEM; $P < 0.05$), whereas *Runx1*, *Runx3*, and *Cbfb* expressions were not significantly altered (Fig. 3*A*). Western blot analysis confirmed a strong increase of RUNX2 on the protein level in whole-lung protein lysates of BLEO-treated mice at d 14 (BLEO fold-change: 3.30 ± 0.46 SEM; $P < 0.01$; Fig. 3*B*). RUNX2 was localized to the alveolar epithelium of fibrotic lungs and to mesenchymal cells (Fig. 3*CI, II*). Similar to human IPF tissue specimens, the quantification of RUNX2-positive cells revealed primarily an increase of double-positive CK/RUNX2 cells (Fig. 3*D* and Supplemental Table 2). Within the αSMA-positive cell population, we also observed a larger increase in RUNX2-negative cells compared with RUNX2-positive cells after bleomycin and compared with PBS control (Fig. 3*D*); however, there was also a small increase in RUNX2-positive fibroblasts. These data urged us to further evaluate the functional role of RUNX2 in both alveolar epithelial and mesenchymal cells.

RUNX2 is upregulated in primary murine ATII cells isolated from fibrotic mice lungs and mediates the expression of fibrosis relevant genes

We isolated primary murine ATII cells of PBS- or bleomycin-treated mice on d 14 after instillation. qPCR analysis revealed a significant upregulation of genes associated with cell proliferation and migration such as *S100a4* (PBS: ΔC_t −3.20 ± 0.16 SEM, BLEO: ΔC_t −0.53 ± 0.31 SEM, $P < 0.001$) and *Cyclin D1* (*Ccnd1*) (PBS ΔC_t 3.77 ± 0.18 SEM, BLEO: ΔC_t 4.45 ± 0.14 SEM, $P < 0.05$), together with significant upregulation of the fibrosis-associated genes *Tnc* (PBS ΔC_t −4.03 ± 0.43 SEM, BLEO: ΔC_t 2.51 ± 0.40 SEM, $P < 0.05$) and *Fn1* (PBS ΔC_t −0.05 ± 0.61 SEM, BLEO: ΔC_t 4.31 ± 0.17 SEM, $P < 0.05$) in ATII cells isolated from bleomycin-treated animals compared to ATII cells isolated from control mice (**Fig. 4*A***), which is in line with previous observations that fibrotic ATII cells are able to express mesenchymal and ECM-related genes (24–26). In parallel, *Runx2* expression in ATII cells was significantly enhanced following bleomycin (PBS ΔC_t −3.37 ± 0.18 SEM, BLEO: ΔC_t −2.03 ± 0.22 SEM, $P < 0.001$). Increased RUNX2 protein levels in fibrotic ATII cells were confirmed by immunofluorescence staining with fibrotic ATII cells exhibiting a strong nuclear expression of RUNX2 (Fig. 4*B*). Of note, nuclear RUNX2 staining has been observed in proliferating fibrotic ATII cells (Fig. 4*BIII*), which have been implicated in disease development and progression

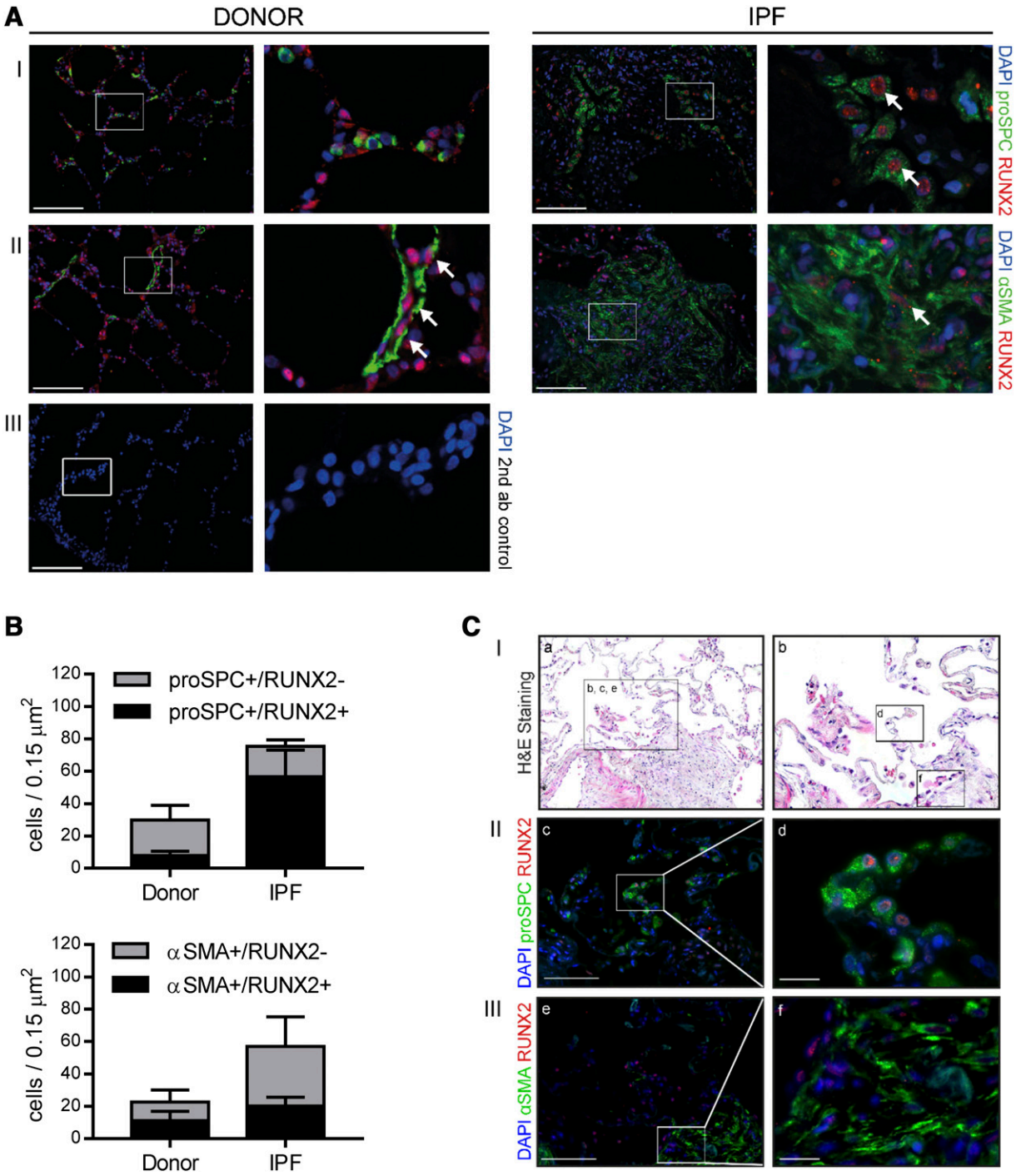

Figure 2. RUNX2 is differentially expressed in ATII cells *vs.* fibroblasts in the IPF lung and mainly colocalizes with proSPC-positive hyperplastic ATII cells. *A*) Immunoflourescence stainings were performed on paraffin sections of donor and IPF lungs. RUNX2 staining is shown in red, costaining with prosurfactant protein C (proSPC; *I*) or α-smooth-muscle actin (αSMA; *II*) in green. DAPI was used to visualize cell nuclei and is shown in blue. Control staining using only secondary antibody and DAPI (*III*). Representative images of 3 donor and 3 IPF lungs. Arrows indicate double stained cells. Scale bars, 100 µm. Arrows indicate double stained cells. *B*) Semiquantitative analysis was performed using 3 representative ×20 images per patient and condition. *C*) Serial sections of an IPF lung showing hyperplastic ATII cells adjacent to a fibroblastic focus. Representative images from H&E staining (*a*, *b*), costaining for proSPC (green) and RUNX2 (red; *c*, *d*) or costaining for αSMA (green) and RUNX2 (red; *e*, *f*). H&E staining is shown to better visualize the underlying tissue architecture. Higher magnifications of white squares in *c*, *e* are shown in *d*, *f*, respectively. Scale bars, 100 µm (*c*, *e*), 20 µm (*d*, *f*).

(27–30). To begin to understand why RUNX2 is upregulated in lung fibrosis, we analyzed RUNX2 expression upon treatment with TGF-β1 or the WNT/β-catenin activator CHIR99021, both of which led to a significant induction of *Runx2* in the ATII cell line A549 (Fig. 4C). Next, we aimed to elucidate the functional role of RUNX2 in the alveolar epithelium and performed RUNX2 knockdown experiments in primary murine ATII cells

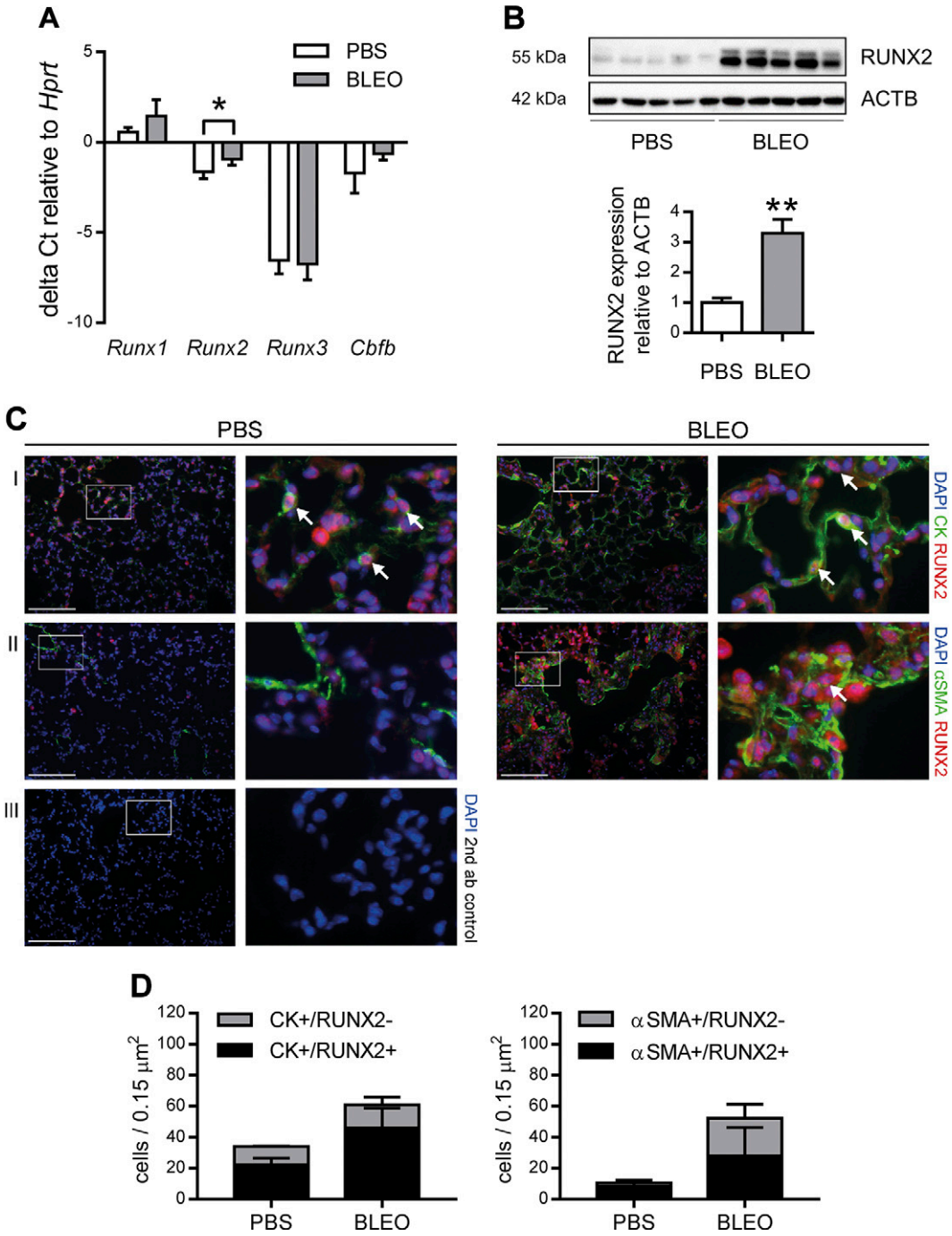

Figure 3. RUNX2 expression is increased in experimental lung fibrosis. *A*) mRNA levels of runt-related transcription (*Runx*) factors and their main interaction partner core-binding factor, β subunit (*Cbfb*) were determined in whole lung extracts from PBS(control)- or bleomycin(BLEO)-challenged mice. Data was normalized to *Hprt* and is shown as ΔC_t, mean ± SEM; $n = 4$ for each group. *B*) Protein expression of RUNX2 in whole lung homogenates on d 14 after instillation of PBS or bleomycin. Densitometric analysis was performed using β-Actin (ACTB) as loading control; $n = 5$ for PBS, $n = 9$ for BLEO. *C*) Representative immunofluorescence stainings of lung sections of bleomycin- or PBS-treated mice. RUNX2 staining is shown in red, costaining with cytokeratin (CK; *I*) or α-smooth-muscle actin (αSMA; *II*) in green. DAPI was used to visualize cell nuclei and is shown in blue. Control staining using only secondary antibody and DAPI (*III*). Higher magnifications of white squares are shown to the right. Arrows indicate double stained cells. Scale bars, 100 µm; $n = 3$ for each group. *D*) Semiquantitative analysis was performed using 3 representative ×20 images per mouse and condition. Statistics: unpaired Student's *t* test (*A*), and Mann-Whitney *U* test (*B*). $^*P < 0.05$, $^{**}P < 0.01$.

isolated on d 14 after bleomycin or PBS instillation using a siRNA approach. RUNX2 knockdown was confirmed by qPCR in the PBS group (fold change: siRUNX2 0.31 ± 0.06 SEM, $P < 0.01$) and in the BLEO group (fold change: siRUNX2 0.42 ± 0.06 SEM, $P < 0.001$) (Fig. 4*D*). Importantly, RUNX2 knockdown led to the reduction of mRNA level of the S100 calcium-binding protein family *S100a4*, which has been implicated in cell migration as well as to

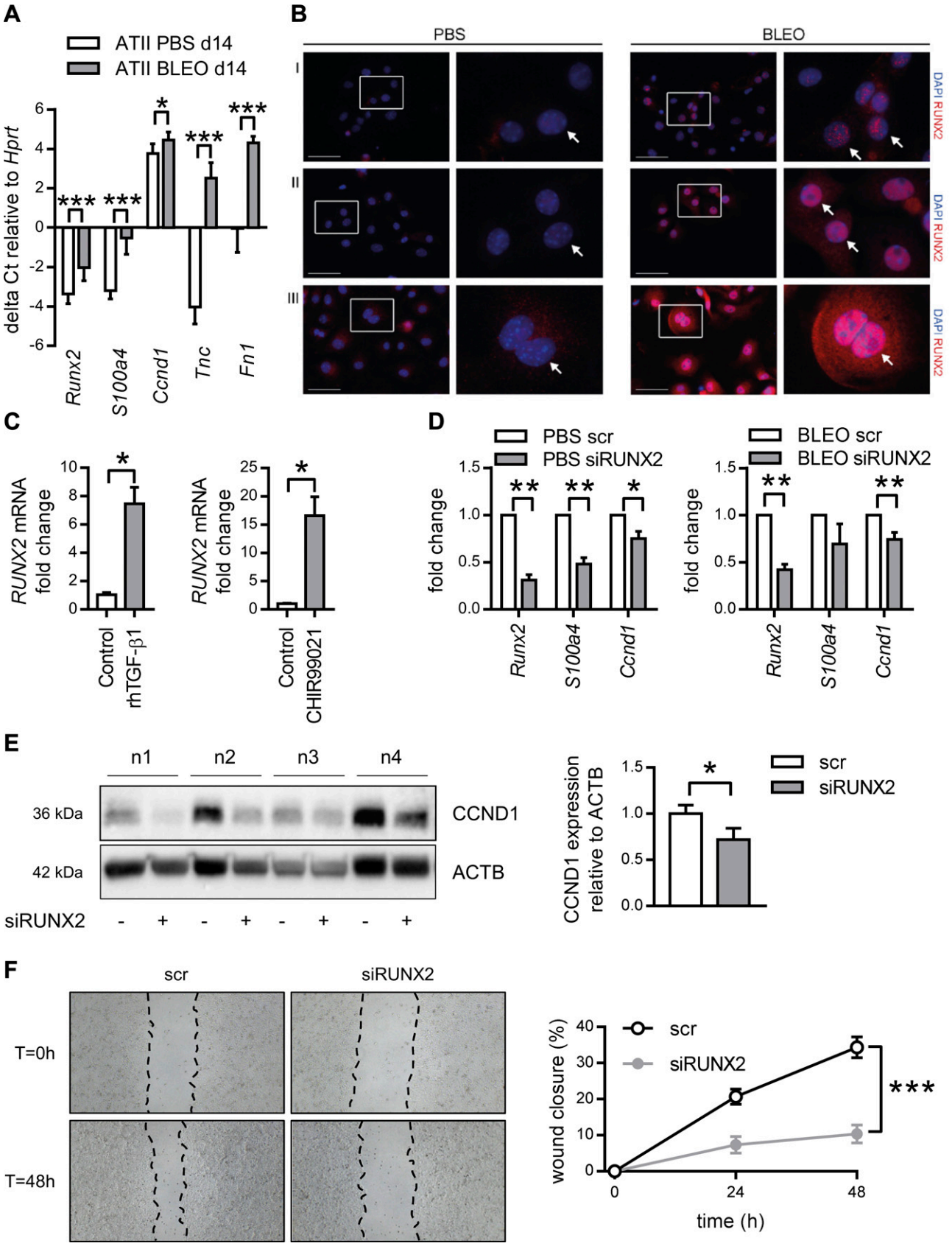

Figure 4. RUNX2 is upregulated in ATII cells isolated from fibrotic mouse lungs and regulates expression of fibrosis associated genes. *A*) On d 14 after instillation of PBS or bleomycin, mice were humanely killed, and ATII cells were isolated. Gene expression was analyzed by qPCR, data was normalized to *Hprt* and is shown as ΔC_t, mean ± SEM; n = 4–8 for PBS, n = 4–9 for BLEO. *B*) Immunofluorescence staining of isolated ATII cells from non-fibrotic and fibrotic mouse lungs. RUNX2 staining is

(*continued on next page*)

the reduction of the cell cycle gene *Ccnd1* in uninjured as well as fibrotic ATII cells (Fig. 4*D*, *E*). Downregulation of CCND1 on protein level upon RUNX2 knockdown was confirmed by Western blotting (Fig. 4*E*). Furthermore, we performed a scratch assay following RUNX2 knockdown on A549 cells. Loss of RUNX2 resulted in a marked inhibition of cell migration (percentage of wound closure at 48 h; scr: 34.33 ± 1.67 SEM, siRUNX2: 10.33 ± 1.45 SEM, $P < 0.001$) (Fig. 4*F*). Together, these data suggest that RUNX2 regulates migratory and potentially hyperplastic behavior of alveolar epithelial cells in lung fibrosis.

Downregulation of RUNX2 in primary human lung fibroblasts promotes myofibroblast differentiation

Semiquantitative analysis of RUNX2 immunofluorescence staining in IPF and experimental lung fibrosis suggested a differential expression of RUNX2 in the fibroblast population upon fibrotic injury. To further confirm these data, we first analyzed a published microarray dataset (GSE17978) where total mRNA, processed right after isolation of fibroblasts from donor or IPF lungs, was analyzed (31). IPF fibroblasts overexpressed several mesenchymal genes such as *COL1A1*, *ACTA2*, *TNC* and *FN1* (relative gene expression: Donors: 0.87 ± 0.05 SEM, IPF patients: 0.55 ± 0.07 SEM, $P < 0.01$) (Supplemental Fig. S3). In line with our observation and in contrast to lung epithelial cells, IPF fibroblasts exhibited a decrease of *RUNX2* mRNA compared with donor fibroblasts (relative gene expression: Donors: 0.87 ± 0.05 SEM, IPF patients: 0.55 ± 0.06 SEM, $P < 0.01$) (**Fig. 5*A***). We further found a significant negative correlation between mRNA levels of *RUNX2* with fibrotic markers, such as *COL1A1* (Pearson $r = -0.52$, $P < 0.05$) and *ACTA2* (Pearson $r = -0.51$, $P < 0.05$) (Fig. 5*A*), suggesting that low RUNX2 levels in fibroblasts promote myofibroblast activation and extracellular matrix deposition. To further proof this association, knockdown of RUNX2 was performed in primary human lung fibroblasts (phLFs) and confirmed by qPCR (fold change at baseline: siRUNX2 0.13 ± 0.01 SEM, $P < 0.01$; fold change after TGF-β1: siRUNX2 0.18 ± 0.06 SEM, $P < 0.01$; Fig. 5*B*). Notably, RUNX2 silencing led to mRNA upregulation of several mesenchymal genes at baseline and upon treatment with TGF-β1, including *COL1A1* (fold change: siRUNX2 1.66 ± 0.23 SEM, $P < 0.05$), *ACTA2* (fold change: siRUNX2 2.57 ± 0.31 SEM, $P < 0.01$) and *TNC* (fold change: siRUNX2 1.59 ± 0.26 SEM, $P < 0.05$). Moreover, only in the presence of TGF-β1, RUNX2 silencing also induced a significant increase of *FN1* expression (fold change: siRUNX2 1.55 ± 0.17 SEM, $P < 0.05$, Fig. 5*B*). Western blotting of whole cell lysates followed by densitometry to ACTB confirmed RUNX2 knockdown (fold change: siRUNX2 0.57 ± 0.05 SEM, $P < 0.05$) and type 1 collagen (COL1) upregulation (fold change: siRUNX2 2.45 ± 0.08 SEM, $P < 0.05$) on protein level (Fig. 5*C*).

DISCUSSION

The runt related transcription factors (RUNX) are a family of 3 genes, essential for cell differentiation, proliferation and lineage specification (8). RUNX2 has been predominantly studied in the context of bone, but has lately gained interest as a driver of different cancer types. RUNX2 is expressed by cancerous mesothelial cells, giving these cells the ability to transform into osteoblast-like cells (32, 33). Interestingly, pleural mesothelial cell plasticity seems to play an important role in the process of pulmonary fibrosis in animal models as well as in IPF (34, 35). While recent studies have reported that RUNX2 might be involved in the pathogenesis of pulmonary hypertension and asthma (36, 37), RUNX2 has not been studied in the context of pulmonary fibrosis and only little is known about RUNX2 function in organ fibrosis in general. The present study demonstrates that RUNX2 is increased in whole lung homogenates from experimental as well as from human IPF tissue specimen with a correlation between *RUNX2* expression level and fibrosis severity. Further, the main partner of RUNX factors CBFB, essential for RUNX2 function (38), is also increased under fibrotic condition compared with control. Nuclear RUNX2 staining was largely observed in proSPC-positive cuboidal shaped alveolar epithelial cells in IPF patients and was also found in isolated ATII cells from fibrotic mice lungs, suggesting a profibrotic role for RUNX2 in ATII cells. Importantly and in contrast to the alveolar epithelial cell compartment, our data suggest that the αSMA-positive myofibroblast population, which increases in IPF lungs, is primarily RUNX2-negative. While an increased expression of RUNX2 in alveolar epithelial cells was associated

shown in red. DAPI was used to visualize cell nuclei and is shown in blue. Representative images of 3 independent experiments are shown. Scale bars, 50 μm. *C*) A549 cells were cultured in presence of TGF-β1 (2 ng/ml), the WNT/β-catenin-activating compound CHIR99021 (2 μM) or corresponding vehicle control for 24 h. Gene expression was analyzed by qPCR, normalized to *Hprt* and displayed as fold change compared to control, means ± SEM; $n = 3$ for each group. *D*) Primary murine ATII cells isolated on d 14 after instillation of PBS or bleomycin were cultured and transfected using a pool of 3 siRNAs targeting *Runx2* mRNA (siRUNX2) or a non-specific scrambled siRNA control (scr). Knockdown was performed for 48 h. Gene expression was displayed as fold change compared to scrambled siRNA control, mean ± SEM; $n = 6$ for PBS groups, $n = 4$–5 for BLEO groups. *E*) Protein expression of CCND1 was determined in cell lysates of scr- or siRUNX2-transfected primary murine ATII cells isolated 14 d after instillation of bleomycin. Densitometric analysis was performed using β-Actin (ACTB) as loading control. *F*) Scratch test performed on A549 cells transfected with a RUNX2–specific siRNA or scrambled siRNA (control). Representative images ($n = 3$) at 0 and 48 h are shown (left). Original magnification, ×4. Wound closure follow-up (right). Data are expressed as percentage of wound closure normalized to wound area at $t = 0$ h, means ± SEM; $n = 3$ for each group. Statistics: unpaired Student's *t* test (*A*, *F*), Mann-Whitney *U* test (*C*, *D*), or paired Student's *t* test (*E*). *$P < 0.05$, **$P < 0.01$, ***$P < 0.001$.

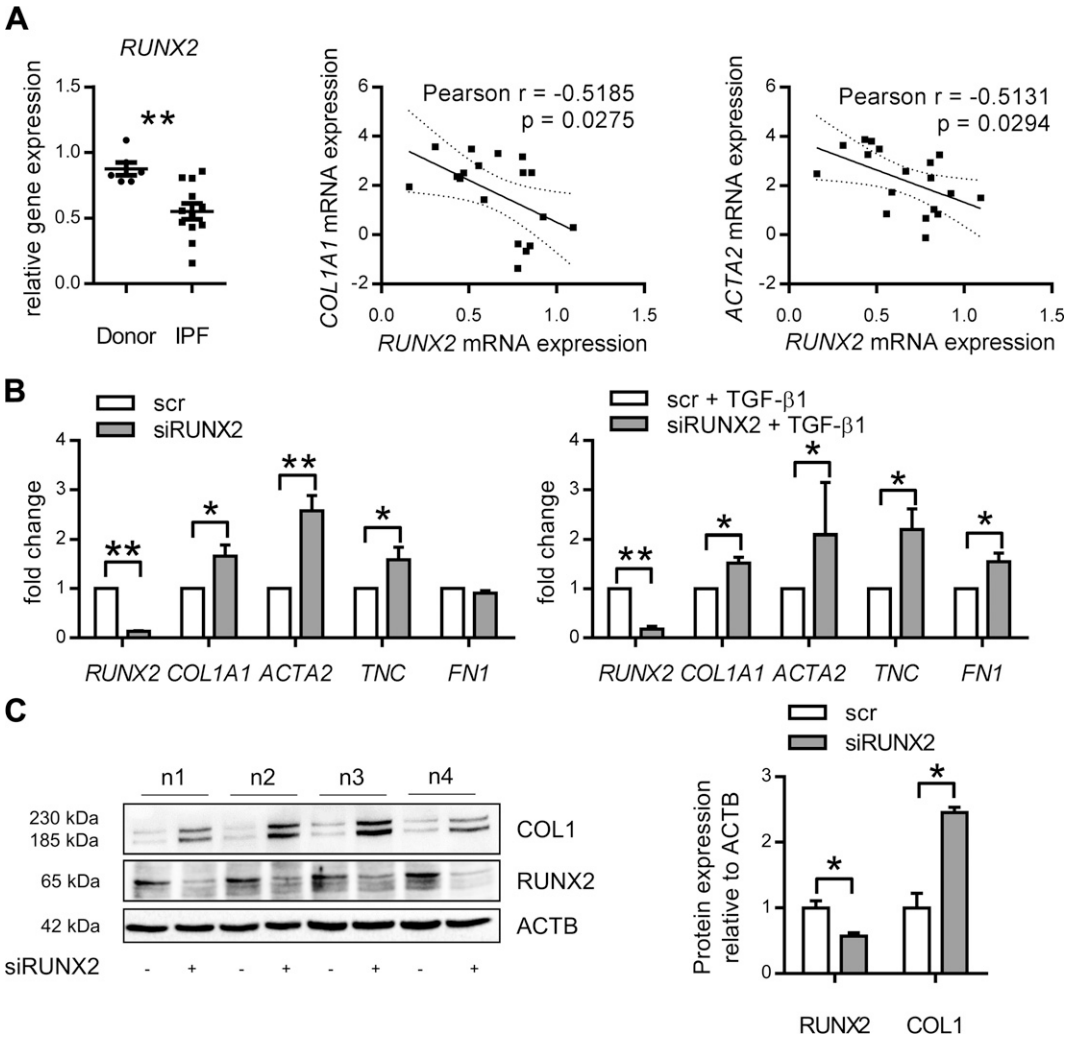

Figure 5. Downregulated RUNX2 in IPF lung fibroblasts promotes myofibroblast differentiation. *A*) Analysis of microarray data published with the accession number GSE17978. Gene expression levels of *RUNX2* were assessed in non-cultured fibroblasts, isolated from donor and IPF lungs and correlated to expression levels of *COL1A1* and *ACTA2*. *B*, *C*) Primary human lung fibroblasts (phLFs) were transfected using a pool of 3 siRNAs targeting *RUNX2* mRNA (siRUNX2) or a non-specific scrambled siRNA control (scr) with or without TGF-β1. Knockdown was performed for 48 h. *B*) Gene expression was analyzed by qPCR, normalized to *HPRT* and displayed as fold change compared to scrambled siRNA control, means ± SEM; $n = 6$ per group. *C*) Protein expression of RUNX2 and collagen1 (COL1) was determined in cell lysates of scr- or siRUNX2-transfected primary human lung fibroblasts. Densitometric analysis was performed using β-Actin (ACTB) as loading control; $n = 4$ per group. Statistics: unpaired Student's *t* test or Pearson *r* was used for correlation analysis (*A*). Mann-Whitney *U* test (*B*, *C*). $^*P < 0.05$, $^{**}P < 0.01$.

with a proliferative and migratory response, we found that reduced *RUNX2* expression in fibroblasts correlated with the upregulation of fibrotic marker genes, such as *COL1A1* and *ACTA2*, thus corroborating our *in vivo* findings in human tissue and suggesting that differential and cell-type dependent RUNX2 expression is involved in fibrogenesis.

Chronic epithelial injury and subsequent hyperplasia of ATII cells with the release of growth factors and cytokines are key features of IPF that contribute to distorted epithelial-mesenchymal crosstalk and (myo)fibroblast function. Several signaling pathways have been demonstrated to be involved in fibrogenesis, among them are the TGF-β and WNT/β-catenin pathways (5). Here, we observed that both, TGF-β and WNT/β-catenin activation induce RUNX2 expression, which is in line with previous reports that reported RUNX2 to be a WNT/β-catenin target gene in osteoblastic cells or mammary epithelium (18, 39). Interplay between RUNX genes and TGF-β signaling can occur at various levels. RUNX2 can modulate the expression of TGF-βRI and/or downstream targets of TGF-β signaling such as SMAD3 (17, 40, 41). Enhanced TGF-β signaling can in turn upregulate RUNX2 on transcriptional level, as observed in this study, and further at the posttranscriptional level through the phosphorylation of RUNX2 by ERK1/2 (8, 42). WNT-induced RUNX2 expression and the subsequent modulation of TGF-βRI by RUNX2 might represent a regulatory cross talk of both signaling pathways and might further serve as a feedback loop enhancing RUNX2 overexpression (17).

We and others previously demonstrated increased proliferative capacity of ATII cells isolated from fibrotic lungs contributing to fibrosis progression (27–30).

Modulation of epithelial cell proliferation has been shown to ameliorate pulmonary fibrosis in rodents (28, 29). In our experiments, loss of RUNX2 in ATII cells led to decreased expression of the proliferation marker *Ccnd1*, further suggesting that increased RUNX2 contributes to fibrogenesis by enhancing epithelial proliferation. In line with these findings, depletion of RUNX2 is associated with reduced regenerative potential in mammary epithelium and interferes with mammary organoid formation (39). Murine RUNX2-negative breast cancers showed reduced levels of CCND1 and Ki-67 expression compared to RUNX2-positive breast cancers (43). Furthermore, in a study with 137 human breast cancer specimen a significant correlation between high RUNX2 levels and high levels of the proliferation marker Ki-67 was demonstrated (44).In addition, it has been shown that RUNX2 is increased in lung cancer and correlates with patients' survival (45, 46). IPF patients have a higher incidence of lung cancer development and several similarities in signaling pathways involved in fibrosis and tumorigenesis have recently been highlighted (47, 48). As such, future studies dissecting the potential role of RUNX2 in these processes is of high interest.

In addition to cell proliferation, several other cellular functions and phenotypes have been associated with alveolar reprogramming in IPF (49). It has been reported that ATII cells isolated from fibrotic lungs are able to partly acquire fibroblast properties, *e.g.*, the enhanced expression of mesenchymal genes like COL1 and αSMA (24–26). RUNX2 has been demonstrated to play a potential role in epithelial to mesenchymal transition (EMT) in the lung epithelial cell line A549, as well as in breast cancer and thyroid carcinoma cells (50–52). While we did not observe differences in epithelial marker gene expression (such as Snai2, E-Cadherin, or tight junction protein 1) upon RUNX2 knockdown (data not shown), we discovered that *S100a4*, a mesenchymal marker and migratory gene, is positively regulated by RUNX2 in ATII cells and that RUNX2 silencing diminished migration properties of A549 cells. S100A4 was initially described as a fibroblast marker upregulated in experimental and human lung fibrosis (53). We found increased *S100a4* expression in fibrotic ATII cells, which might indicate reprogramming of these cells (28). Interestingly, increased S100A4 staining has been demonstrated in TTF1-positive epithelial cells in experimental lung fibrosis (54). Further studies demonstrated that S100A4-positive fibroblasts were partly derived from lung epithelium after bleomycin injury, however they rarely showed a myofibroblast phenotype (55). RUNX2-dependent regulation of S100A4 has been linked to a migratory profile associated with metastasis in breast and prostate cancer (40, 51). Thus, it is possible that RUNX2 initiates a process of reprogramming in alveolar epithelial cells and exerts a migratory effect through induction of S100A4 in injured alveolar epithelium. This concept is in line with a recent study demonstrating that S100A4 positive cells, which surround fibroblastic foci in IPF, are highly proliferative and constitute an active fibrotic front (56).

The accumulation of activated αSMA-positive myofibroblasts is another pathologic feature of IPF. Unexpectedly, we found a decreased expression of RUNX2 in fibrotic fibroblasts compared to fibrotic alveolar epithelial cells and observed an increase in RUNX2-negative αSMA-positive myofibroblasts in IPF, indicating that loss of RUNX2 is involved in profibrotic function of these cells. In line with this, our data revealed that RUNX2 silencing in fibroblasts enhanced myofibroblast differentiation through induction of *COL1A1*, *ACTA2* and *TNC* genes. Notably, we analyzed a publicly available microarray data set comparing IPF and donor fibroblasts, in which we found that loss of *RUNX2* correlated with increase in *COL1A1* and *ACTA2* expression. Consistent with our findings, it has been reported that downregulation of RUNX1 is necessary for the differentiation of mesenchymal stem cells toward myofibroblasts. The authors reported that knockdown of RUNX1 led to upregulation of myofibroblast markers TNC and ACTA2 (57). Since we excluded alterations in RUNX1 expression in our studies, this indicates a potentially overlapping function of RUNX genes. Furthermore, RUNX2 has been shown to suppress the expression of type 1 collagen in non-osseous mesenchymal cells (58). Importantly, upregulation of αSMA, COL1 and COL3 have been reported in a RUNX2 heterozygous knockout mice subjected to a ureteral obstruction model of kidney fibrosis (41). It will be important in future studies to elucidate the cell-specific contribution of RUNX2 expression in a similar experimental lung fibrosis model *in vivo*.

Our findings of differential RUNX2 expression in experimental and human IPF raises the question how RUNX2 expression is regulated and which mechanisms are involved in either up- or downregulating RUNX2 in different cell types. The latter is of high interest, as we observed that both TGF-β1 as well as WNT/β-catenin activation induces a robust expression of RUNX2 in ATII cells. Cell-specific changes within the (epi)genetic profile of different cell types might result in a different RUNX2 expression. Moreover, the availability of secreted profibrotic mediators might be distinct within the local microenvironment between alveolar epithelial cells and fibroblasts. With respect to WNT signaling, which can be divided into two main pathways (a canonical WNT/β-catenin signaling and a non-canonical β-catenin independent pathway) (59), we and others have provided evidence of a differential WNT ligand signature, with an increase of non-canonical WNT ligand (such as WNT5A and WNT5B) expression by fibroblasts (60, 61). This altered signaling pattern might act differentially on several cell types depending on the expression of specific WNT surface receptors, which needs to be further investigated in future studies. The transcription factor TWIST1 represents another potential regulator of RUNX2 expression in fibroblasts. TWIST1 has been demonstrated to downregulate RUNX2 expression in zebrafish embryos (62) as well as in human mesenchymal stem cells by directly binding to the RUNX2-promotor (63). Interestingly, several groups have shown that TWIST1 is expressed in human IPF as well as in murine models of pulmonary fibrosis. Two studies demonstrated TWIST1 staining in alveolar epithelial cells and fibroblasts, whereas another study exclusively located TWIST1 to fibrotic fibroblasts (64–66). Therefore, increased

TWIST1 expression in fibrotic fibroblasts might be responsible of downregulation of RUNX2, leading to myofibroblast differentiation and increased ECM deposition.

Based on our findings, we hypothesize that the total amount of RUNX2 in the fibrotic lung primarily reflects the increased expression in injured and hyperplastic alveolar epithelial cells, which do express substantial amounts of RUNX2. In line with this, we found that IPF patients with higher *RUNX2* mRNA expression in whole lung homogenates exhibited worse prognostic markers, for instance reduced DLCO and increased biomarkers *MMP7*, *SPP1* indicating that RUNX2 level might serve as novel surrogate marker of IPF progression. The downregulation of RUNX2 in fibrotic fibroblasts, however, promoting differentiation into myofibroblasts, is masked in total lung homogenates, further highlighting the importance of cell-specific analysis. One limitation of this study resides in the lack of *in vivo* evidences concerning the cell-specific contribution of RUNX2 to the development and progression of lung fibrosis. This could be addressed using transgenic mice with conditional and cell-specific deletion of RUNX2 and would help to further identify cell-specific RUNX2 activator/repressor that could be further investigated as therapeutic targets for IPF. FJ

ACKNOWLEDGMENTS

The authors are grateful to all members of the M.G. Laboratory for stimulating discussions. The authors thank Darcy E. Wagner for helping with dataset analysis, Nadine Adam, Anastasia van den Berg, Julia Kipp and Marlene Stein (all of the Comprehensive Pneumology Center Munich, Ludwig Maximillians University) for excellent technical assistance and Nicole Manning (University of Colorado) for proofreading the manuscript. This work was funded by grants from the German Center of Lung Research and the Helmholtz Association. Helmholtz Center Munich and University of Giessen Lung Center are members of the German Center for Lung Research. O.B. is supported by a postdoctoral fellowship from the European Respiratory Society and the European Molecular Biology Organization (Fellowship ERS LTRF 2016-7481). The authors declare no conflicts of interest.

AUTHOR CONTRIBUTIONS

C. Mümmler, S. Hermann, and M. Königshoff designed the research project; C. Mümmler, O. Burgy, S. Hermann, K. Mutze, and M. Königshoff planned and performed experiments and analyzed the data; A. Günther contributed to tissue specimen and clinical expertise; C. Mümmler, O. Burgy, and M. Königshoff wrote the manuscript; and all authors approved the final version of the manuscript.

REFERENCES

1. Raghu, G., Collard, H. R., Egan, J. J., Martinez, F. J., Behr, J., Brown, K. K., Colby, T. V., Cordier, J. F., Flaherty, K. R., Lasky, J. A., Lynch, D. A., Ryu, J. H., Swigris, J. J., Wells, A. U., Ancochea, J., Bouros, D., Carvalho, C., Costabel, U., Ebina, M., Hansell, D. M., Johkoh, T., Kim, D. S., King, T. E., Jr., Kondoh, Y., Myers, J., Müller, N. L., Nicholson, A. G., Richeldi, L., Selman, M., Dudden, R. F., Griss, B. S., Protzko, S. L., and Schünemann, H. J.; ATS/ERS/JRS/ALAT Committee on Idiopathic Pulmonary Fibrosis. (2011) An official ATS/ERS/JRS/ALAT statement: idiopathic pulmonary fibrosis: evidence-based guidelines for diagnosis and management. *Am. J. Respir. Crit. Care Med.* **183**, 788–824
2. King, T. E., Jr., Pardo, A., and Selman, M. (2011) Idiopathic pulmonary fibrosis. *Lancet* **378**, 1949–1961
3. Fernandez, I. E., and Eickelberg, O. (2012) New cellular and molecular mechanisms of lung injury and fibrosis in idiopathic pulmonary fibrosis. *Lancet* **380**, 680–688
4. Selman, M., and Pardo, A. (2006) Role of epithelial cells in idiopathic pulmonary fibrosis: from innocent targets to serial killers. *Proc. Am. Thorac. Soc.* **3**, 364–372
5. Baarsma, H. A., and Königshoff, M. (2017) 'WNT-er is coming': WNT signalling in chronic lung diseases. *Thorax* **72**, 746–759
6. King, T. E., Jr., Bradford, W. Z., Castro-Bernardini, S., Fagan, E. A., Glaspole, I., Glassberg, M. K., Gorina, E., Hopkins, P. M., Kardatzke, D., Lancaster, L., Lederer, D. J., Nathan, S. D., Pereira, C. A., Sahn, S. A., Sussman, R., Swigris, J. J., and Noble, P. W.; ASCEND Study Group. (2014) A phase 3 trial of pirfenidone in patients with idiopathic pulmonary fibrosis. *N. Engl. J. Med.* **370**, 2083–2092; erratum: **371**, 1172
7. Richeldi, L., du Bois, R. M., Raghu, G., Azuma, A., Brown, K. K., Costabel, U., Cottin, V., Flaherty, K. R., Hansell, D. M., Inoue, Y., Kim, D. S., Kolb, M., Nicholson, A. G., Noble, P. W., Selman, M., Taniguchi, H., Brun, M., Le Maulf, F., Girard, M., Stowasser, S., Schlenker-Herceg, R., Disse, B., and Collard, H. R.; INPULSIS Trial Investigators. (2014) Efficacy and safety of nintedanib in idiopathic pulmonary fibrosis. *N. Engl. J. Med.* **370**, 2071–20822082; erratum: 2015
8. Blyth, K., Cameron, E. R., and Neil, J. C. (2005) The RUNX genes: gain or loss of function in cancer. *Nat. Rev. Cancer* **5**, 376–387
9. Tahirov, T. H., Inoue-Bungo, T., Morii, H., Fujikawa, A., Sasaki, M., Kimura, K., Shiina, M., Sato, K., Kumasaka, T., Yamamoto, M., Ishii, S., and Ogata, K. (2001) Structural analyses of DNA recognition by the AML1/Runx-1 Runt domain and its allosteric control by CBFbeta. *Cell* **104**, 755–767; erratum: 105, 291
10. Huang, X., Peng, J. W., Speck, N. A., and Bushweller, J. H. (1999) Solution structure of core binding factor β and map of the CBFα binding site. *Nat. Struct. Biol.* **6**, 624–627
11. Pratap, J., Lian, J. B., Javed, A., Barnes, G. L., van Wijnen, A. J., Stein, J. L., and Stein, G. S. (2006) Regulatory roles of Runx2 in metastatic tumor and cancer cell interactions with bone. *Cancer Metastasis Rev.* **25**, 589–600
12. Chuang, L. S., Ito, K., and Ito, Y. (2013) RUNX family: regulation and diversification of roles through interacting proteins. *Int. J. Cancer* **132**, 1260–1271
13. Okuda, T., van Deursen, J., Hiebert, S. W., Grosveld, G., and Downing, J. R. (1996) AML1, the target of multiple chromosomal translocations in human leukemia, is essential for normal fetal liver hematopoiesis. *Cell* **84**, 321–330
14. Lee, K. S., Lee, Y. S., Lee, J. M., Ito, K., Cinghu, S., Kim, J. H., Jang, J. W., Li, Y. H., Goh, Y. M., Chi, X. Z., Wee, H., Lee, H. W., Hosoya, A., Chung, J. H., Jang, J. J., Kundu, J. K., Surh, Y. J., Kim, W. J., Ito, Y., Jung, H. S., and Bae, S. C. (2010) Runx3 is required for the differentiation of lung epithelial cells and suppression of lung cancer. *Oncogene* **29**, 3349–3361
15. Otto, F., Thornell, A. P., Crompton, T., Denzel, A., Gilmour, K. C., Rosewell, I. R., Stamp, G. W., Beddington, R. S., Mundlos, S., Olsen, B. R., Selby, P. B., and Olsen, M. J. (1997) Cbfa1, a candidate gene for cleidocranial dysplasia syndrome, is essential for osteoblast differentiation and bone development. *Cell* **89**, 765–771
16. Ito, Y., and Miyazono, K. (2003) RUNX transcription factors as key targets of TGF-beta superfamily signaling. *Curr. Opin. Genet. Dev.* **13**, 43–47
17. McCarthy, T. L., and Centrella, M. (2010) Novel links among Wnt and TGF-beta signaling and Runx2. *Mol. Endocrinol.* **24**, 587–597
18. Gaur, T., Lengner, C. J., Hovhannisyan, H., Bhat, R. A., Bodine, P. V., Komm, B. S., Javed, A., van Wijnen, A. J., Stein, J. L., Stein, G. S., and Lian, J. B. (2005) Canonical WNT signaling promotes osteogenesis by directly stimulating Runx2 gene expression. *J. Biol. Chem.* **280**, 33132–33140
19. Mutze, K., Vierkotten, S., Milosevic, J., Eickelberg, O., and Königshoff, M. (2015) Enolase 1 (ENO 1) and protein disulfide-isomerase associated 3 (PDIA 3) regulate Wnt/β-catenin-driven trans-differentiation of murine alveolar epithelial cells. *Dis. Model. Mech.* **8**, 877–890

20. Klee, S., Lehmann, M., Wagner, D. E., Baarsma, H. A., and Königshoff, M. (2016) WISP1 mediates IL-6-dependent proliferation in primary human lung fibroblasts. *Sci. Rep.* **6**, 20547
21. Bellaye, P. S., Burgy, O., Colas, J., Fabre, A., Marchal-Somme, J., Crestani, B., Kolb, M., Camus, P., Garrido, C., and Bonniaud, P. (2015) Antifibrotic role of αB-crystallin inhibition in pleural and subpleural fibrosis. *Am. J. Respir. Cell Mol. Biol.* **52**, 244–252
22. White, E. S., Xia, M., Murray, S., Dyal, R., Flaherty, C. M., Flaherty, K. R., Moore, B. B., Cheng, L., Doyle, T. J., Villalba, J., Dellaripa, P. F., Rosas, I. O., Kurtis, J. D., and Martinez, F. J. (2016) Plasma surfactant protein-D, matrix metalloproteinase-7, and osteopontin index distinguishes idiopathic pulmonary fibrosis from other idiopathic interstitial pneumonias. *Am. J. Respir. Crit. Care Med.* **194**, 1242–1251
23. Jenkins, R. G., Moore, B. B., Chambers, R. C., Eickelberg, O., Königshoff, M., Kolb, M., Laurent, G. J., Nanthakumar, C. B., Olman, M. A., Pardo, A., Selman, M., Sheppard, D., Sime, P. J., Tager, A. M., Tatler, A. L., Thannickal, V. J., and White, E. S.; ATS Assembly on Respiratory Cell and Molecular Biology. (2017) An official American thoracic society workshop report: use of animal models for the preclinical assessment of potential therapies for pulmonary fibrosis. *Am. J. Respir. Cell Mol. Biol.* **56**, 667–679
24. Yang, J., Wheeler, S. E., Velikoff, M., Kleaveland, K. R., LaFemina, M. J., Frank, J. A., Chapman, H. A., Christensen, P. J., and Kim, K. K. (2013) Activated alveolar epithelial cells initiate fibrosis through secretion of mesenchymal proteins. *Am. J. Pathol.* **183**, 1559–1570
25. Kim, K. K., Kugler, M. C., Wolters, P. J., Robillard, L., Galvez, M. G., Brumwell, A. N., Sheppard, D., and Chapman, H. A. (2006) Alveolar epithelial cell mesenchymal transition develops in vivo during pulmonary fibrosis and is regulated by the extracellular matrix. *Proc. Natl. Acad. Sci. USA* **103**, 13180–13185
26. Marmai, C., Sutherland, R. E., Kim, K. K., Dolganov, G. M., Fang, X., Kim, S. S., Jiang, S., Golden, J. A., Hoopes, C. W., Matthay, M. A., Chapman, H. A., and Wolters, P. J. (2011) Alveolar epithelial cells express mesenchymal proteins in patients with idiopathic pulmonary fibrosis. *Am. J. Physiol. Lung Cell. Mol. Physiol.* **301**, L71–L78
27. Königshoff, M., and Bonniaud, P. (2014) Live and let die: targeting alveolar epithelial cell proliferation in pulmonary fibrosis. *Am. J. Respir. Crit. Care Med.* **190**, 1339–1341
28. Königshoff, M., Kramer, M., Balsara, N., Wilhelm, J., Amarie, O. V., Jahn, A., Rose, F., Fink, L., Seeger, W., Schaefer, L., Günther, A., and Eickelberg, O. (2009) WNT1-inducible signaling protein-1 mediates pulmonary fibrosis in mice and is upregulated in humans with idiopathic pulmonary fibrosis. *J. Clin. Invest.* **119**, 772–787
29. Pullamsetti, S. S., Savai, R., Dumitrascu, R., Dahal, B. K., Wilhelm, J., Konigshoff, M., Zakrzewicz, D., Ghofrani, H. A., Weissmann, N., Eickelberg, O., Guenther, A., Leiper, J., Seeger, W., Grimminger, F., and Schermuly, R. T. (2011) The role of dimethylarginine dimethylaminohydrolase in idiopathic pulmonary fibrosis. *Sci. Transl. Med.* **3**, 87ra53
30. Weng, T., Poth, J. M., Karmouty-Quintana, H., Garcia-Morales, L. J., Melicoff, E., Luo, F., Chen, N. Y., Evans, C. M., Bunge, R. R., Bruckner, B. A., Loebe, M., Volcik, K. A., Eltzschig, H. K., and Blackburn, M. R. (2014) Hypoxia-induced deoxycytidine kinase contributes to epithelial proliferation in pulmonary fibrosis. *Am. J. Respir. Crit. Care Med.* **190**, 1402–1412
31. Emblom-Callahan, M. C., Chhina, M. K., Shlobin, O. A., Ahmad, S., Reese, E. S., Iyer, E. P., Cox, D. N., Brenner, R., Burton, N. A., Grant, G. M., and Nathan, S. D. (2010) Genomic phenotype of non-cultured pulmonary fibroblasts in idiopathic pulmonary fibrosis. *Genomics* **96**, 134–145
32. Lansley, S. M., Searles, R. G., Hoi, A., Thomas, C., Moneta, H., Herrick, S. E., Thompson, P. J., Newman, M., Sterrett, G. F., Prêle, C. M., and Mutsaers, S. E. (2011) Mesothelial cell differentiation into osteoblast- and adipocyte-like cells. *J. Cell. Mol. Med.* **15**, 2095–2105
33. Lansley, S. M., Pedersen, B., Robinson, C., Searles, R. G., Sterrett, G., van Bruggen, I., Lake, R. A., Mutsaers, S. E., and Prêle, C. M. (2016) A subset of malignant mesothelioma tumors retain osteogenic potential. *Sci. Rep.* **6**, 36349
34. Burgy, O., Bellaye, P. S., Causse, S., Beltramo, G., Wettstein, G., Boutanquoi, P. M., Goirand, F., Garrido, C., and Bonniaud, P. (2016) Pleural inhibition of the caspase-1/IL-1β pathway diminishes profibrotic lung toxicity of bleomycin. *Respir. Res.* **17**, 162
35. Nasreen, N., Mohammed, K. A., Mubarak, K. K., Baz, M. A., Akindipe, O. A., Fernandez-Bussy, S., and Antony, V. B. (2009) Pleural mesothelial cell transformation into myofibroblasts and haptotactic migration in response to TGF-beta1 in vitro. *Am. J. Physiol. Lung Cell. Mol. Physiol.* **297**, L115–L124
36. Ruffenach, G., Chabot, S., Tanguay, V. F., Courboulin, A., Boucherat, O., Potus, F., Meloche, J., Pflieger, A., Breuils-Bonnet, S., Nadeau, V., Paradis, R., Tremblay, E., Girerd, B., Hautefort, A., Montani, D., Fadel, E., Dorfmuller, P., Humbert, M., Perros, F., Paulin, R., Provencher, S., and Bonnet, S. (2016) Role for runt-related transcription factor 2 in proliferative and calcified vascular lesions in pulmonary arterial hypertension. *Am. J. Respir. Crit. Care Med.* **194**, 1273–1285
37. Shi, N., Zhang, J., and Chen, S. Y. (2017) Runx2, a novel regulator for goblet cell differentiation and asthma development. *FASEB J.* **31**, 412–420
38. Ito, Y., Bae, S. C., and Chuang, L. S. (2015) The RUNX family: developmental regulators in cancer. *Nat. Rev. Cancer* **15**, 81–95
39. Ferrari, N., Riggio, A. I., Mason, S., McDonald, L., King, A., Higgins, T., Rosewell, I., Neil, J. C., Smalley, M. J., Sansom, O. J., Morris, J., Cameron, E. R., and Blyth, K. (2015) Runx2 contributes to the regenerative potential of the mammary epithelium. *Sci. Rep.* **5**, 15658
40. Baniwal, S. K., Khalid, O., Gabet, Y., Shah, R. R., Purcell, D. J., Mav, D., Kohn-Gabet, A. E., Shi, Y., Coetzee, G. A., and Frenkel, B. (2010) Runx2 transcriptome of prostate cancer cells: insights into invasiveness and bone metastasis. *Mol. Cancer* **9**, 258
41. Kim, J. I., Jang, H. S., Jeong, J. H., Noh, M. R., Choi, J. Y., and Park, K. M. (2013) Defect in Runx2 gene accelerates ureteral obstruction-induced kidney fibrosis via increased TGF-β signaling pathway. *Biochim. Biophys. Acta* **1832**, 1520–1527
42. Ji, C., Casinghino, S., Chang, D. J., Chen, Y., Javed, A., Ito, Y., Hiebert, S. W., Lian, J. B., Stein, G. S., McCarthy, T. L., and Centrella, M. (1998) CBFa(AML/PEBP2)-related elements in the TGF-β type I receptor promoter and expression with osteoblast differentiation. *J. Cell. Biochem.* **69**, 353–363
43. Owens, T. W., Rogers, R. L., Best, S., Ledger, A., Mooney, A. M., Ferguson, A., Shore, P., Swarbrick, A., Ormandy, C. J., Simpson, P. T., Carroll, J. S., Visvader, J., and Naylor, M. J. (2014) Runx2 is a novel regulator of mammary epithelial cell fate in development and breast cancer. *Cancer Res.* **74**, 5277–5286
44. Onodera, Y., Miki, Y., Suzuki, T., Takagi, K., Akahira, J., Sakyu, T., Watanabe, M., Inoue, S., Ishida, T., Ohuchi, N., and Sasano, H. (2010) Runx2 in human breast carcinoma: its potential roles in cancer progression. *Cancer Sci.* **101**, 2670–2675
45. Li, H., Zhou, R. J., Zhang, G. Q., and Xu, J. P. (2013) Clinical significance of RUNX2 expression in patients with nonsmall cell lung cancer: a 5-year follow-up study. *Tumour Biol.* **34**, 1807–1812
46. Chang, C. H., Fan, T. C., Yu, J. C., Liao, G. S., Lin, Y. C., Shih, A. C., Li, W. H., and Yu, A. L. (2014) The prognostic significance of RUNX2 and miR-10a/10b and their inter-relationship in breast cancer. *J. Transl. Med.* **12**, 257
47. Königshoff, M. (2011) Lung cancer in pulmonary fibrosis: tales of epithelial cell plasticity. *Respiration* **81**, 353–358
48. Horowitz, J. C., Osterholzer, J. J., Marazioti, A., and Stathopoulos, G. T. (2016) "Scar-cinoma": viewing the fibrotic lung mesenchymal cell in the context of cancer biology. *Eur. Respir. J.* **47**, 1842–1854
49. Blackwell, T. S., Tager, A. M., Borok, Z., Moore, B. B., Schwartz, D. A., Anstrom, K. J., Bar-Joseph, Z., Bitterman, P., Blackburn, M. R., Bradford, W., Brown, K. K., Chapman, H. A., Collard, H. R., Cosgrove, G. P., Deterding, R., Doyle, R., Flaherty, K. R., Garcia, C. K., Hagood, J. S., Henke, C. A., Herzog, E., Hogaboam, C. M., Horowitz, J. C., King, T. E., Jr., Loyd, J. E., Lawson, W. E., Marsh, C. B., Noble, P. W., Noth, I., Sheppard, D., Olsson, J., Ortiz, L. A., O'Riordan, T. G., Oury, T. D., Raghu, G., Roman, J., Sime, P. J., Sisson, T. H., Tschumperlin, D., Violette, S. M., Weaver, T. E., Wells, R. G., White, E. S., Kaminski, N., Martinez, F. J., Wynn, T. A., Thannickal, V. J., and Eu, J. P. (2014) Future directions in idiopathic pulmonary fibrosis research. An NHLBI workshop report. *Am. J. Respir. Crit. Care Med.* **189**, 214–222
50. Hsu, Y. L., Huang, M. S., Yang, C. J., Hung, J. Y., Wu, L. Y., and Kuo, P. L. (2011) Lung tumor-associated osteoblast-derived bone morphogenetic protein-2 increased epithelial-to-mesenchymal transition of cancer by Runx2/Snail signaling pathway. *J. Biol. Chem.* **286**, 37335–37346
51. Chimge, N. O., Baniwal, S. K., Little, G. H., Chen, Y. B., Kahn, M., Tripathy, D., Borok, Z., and Frenkel, B. (2011) Regulation of breast cancer metastasis by Runx2 and estrogen signaling: the role of SNAI2. *Breast Cancer Res.* **13**, R127
52. Niu, D. F., Kondo, T., Nakazawa, T., Oishi, N., Kawasaki, T., Mochizuki, K., Yamane, T., and Katoh, R. (2012) Transcription factor Runx2 is a regulator of epithelial-mesenchymal transition and invasion in thyroid carcinomas. *Lab. Invest.* **92**, 1181–1190

53. Lawson, W. E., Polosukhin, V. V., Zoia, O., Stathopoulos, G. T., Han, W., Plieth, D., Loyd, J. E., Neilson, E. G., and Blackwell, T. S. (2005) Characterization of fibroblast-specific protein 1 in pulmonary fibrosis. *Am. J. Respir. Crit. Care Med.* **171**, 899–907
54. Pozharskaya, V., Torres-González, E., Rojas, M., Gal, A., Amin, M., Dollard, S., Roman, J., Stecenko, A. A., and Mora, A. L. (2009) Twist: a regulator of epithelial-mesenchymal transition in lung fibrosis. *PLoS One* **4**, e7559
55. Tanjore, H., Xu, X. C., Polosukhin, V. V., Degryse, A. L., Li, B., Han, W., Sherrill, T. P., Plieth, D., Neilson, E. G., Blackwell, T. S., and Lawson, W. E. (2009) Contribution of epithelial-derived fibroblasts to bleomycin-induced lung fibrosis. *Am. J. Respir. Crit. Care Med.* **180**, 657–665
56. Xia, H., Gilbertsen, A., Herrera, J., Racila, E., Smith, K., Peterson, M., Griffin, T., Benyumov, A., Yang, L., Bitterman, P. B., and Henke, C. A. (2017) Calcium-binding protein S100A4 confers mesenchymal progenitor cell fibrogenicity in idiopathic pulmonary fibrosis. *J. Clin. Invest.* **127**, 2586–2597
57. Kim, W., Barron, D. A., San Martin, R., Chan, K. S., Tran, L. L., Yang, F., Ressler, S. J., and Rowley, D. R. (2014) RUNX1 is essential for mesenchymal stem cell proliferation and myofibroblast differentiation. *Proc. Natl. Acad. Sci. USA* **111**, 16389–16394
58. Tsuji, K., Ito, Y., and Noda, M. (1998) Expression of the PEBP2alphaA/AML3/CBFA1 gene is regulated by BMP4/7 heterodimer and its overexpression suppresses type I collagen and osteocalcin gene expression in osteoblastic and nonosteoblastic mesenchymal cells. *Bone* **22**, 87–92
59. Baarsma, H. A., Königshoff, M., and Gosens, R. (2013) The WNT signaling pathway from ligand secretion to gene transcription: molecular mechanisms and pharmacological targets. *Pharmacol. Ther.* **138**, 66–83
60. Baarsma, H. A., Skronska-Wasek, W., Mutze, K., Ciolek, F., Wagner, D. E., John-Schuster, G., Heinzelmann, K., Günther, A., Bracke, K. R., Dagouassat, M., Boczkowski, J., Brusselle, G. G., Smits, R., Eickelberg, O., Yildirim, A. O., and Königshoff, M. (2017) Noncanonical WNT-5A signaling impairs endogenous lung repair in COPD. *J. Exp. Med.* **214**, 143–163; erratum: 2017
61. van Dijk, E. M., Menzen, M. H., Spanjer, A. I., Middag, L. D., Brandsma, C. A., and Gosens, R. (2016) Noncanonical WNT-5B signaling induces inflammatory responses in human lung fibroblasts. *Am. J. Physiol. Lung Cell. Mol. Physiol.* **310**, L1166–L1176
62. Yang, D. C., Tsai, C. C., Liao, Y. F., Fu, H. C., Tsay, H. J., Huang, T. F., Chen, Y. H., and Hung, S. C. (2011) Twist controls skeletal development and dorsoventral patterning by regulating runx2 in zebrafish. *PLoS One* **6**, e27324
63. Yang, D. C., Yang, M. H., Tsai, C. C., Huang, T. F., Chen, Y. H., and Hung, S. C. (2011) Hypoxia inhibits osteogenesis in human mesenchymal stem cells through direct regulation of RUNX2 by TWIST. *PLoS One* **6**, e23965
64. Bridges, R. S., Kass, D., Loh, K., Glackin, C., Borczuk, A. C., and Greenberg, S. (2009) Gene expression profiling of pulmonary fibrosis identifies Twist1 as an antiapoptotic molecular "rectifier" of growth factor signaling. *Am. J. Pathol.* **175**, 2351–2361
65. Pozharskaya, V., Torres-González, E., Rojas, M., Gal, A., Amin, M., Dollard, S., Roman, J., Stecenko, A. A., and Mora, A. L. (2009) Twist: a regulator of epithelial-mesenchymal transition in lung fibrosis. *PLoS One* **4**, e7559
66. Lomas, N. J., Watts, K. L., Akram, K. M., Forsyth, N. R., and Spiteri, M. A. (2012) Idiopathic pulmonary fibrosis: immunohistochemical analysis provides fresh insights into lung tissue remodelling with implications for novel prognostic markers. *Int. J. Clin. Exp. Pathol.* **5**, 58–71

Received for publication May 25, 2017.
Accepted for publication September 18, 2017.

THE FASEB JOURNAL
The Journal of the Federation of American Societies for Experimental Biology

Cell-specific expression of runt-related transcription factor 2 contributes to pulmonary fibrosis

Carlo Mümmler, Olivier Burgy, Sarah Hermann, et al.

FASEB J published online October 6, 2017
Access the most recent version at doi:10.1096/fj.201700482R